Accepted Manuscript

Synthesis and electrochemical performance of an imidazolium based Li salt as electrolyte with Li fluorinated sulfonylimides as additives for Li-Ion batteries

Faiz Ahmed, Md. Mahbubur Rahman, Sabuj Chandra Sutradhar, Nasrin Siraj Lopa, Taewook Ryu, Sujin Yoon, Inhwan Choi, Yonghoon Lee, Whangi Kim

PII: S0013-4686(19)30283-X

DOI: https://doi.org/10.1016/j.electacta.2019.02.040

Reference: EA 33631

To appear in: *Electrochimica Acta*

Received Date: 27 November 2018

Revised Date: 8 February 2019

Accepted Date: 8 February 2019

Please cite this article as: F. Ahmed, M.M. Rahman, S.C. Sutradhar, N.S. Lopa, T. Ryu, S. Yoon, I. Choi, Y. Lee, W. Kim, Synthesis and electrochemical performance of an imidazolium based Li salt as electrolyte with Li fluorinated sulfonylimides as additives for Li-Ion batteries, *Electrochimica Acta* (2019), doi: https://doi.org/10.1016/j.electacta.2019.02.040.

Graphical abstract

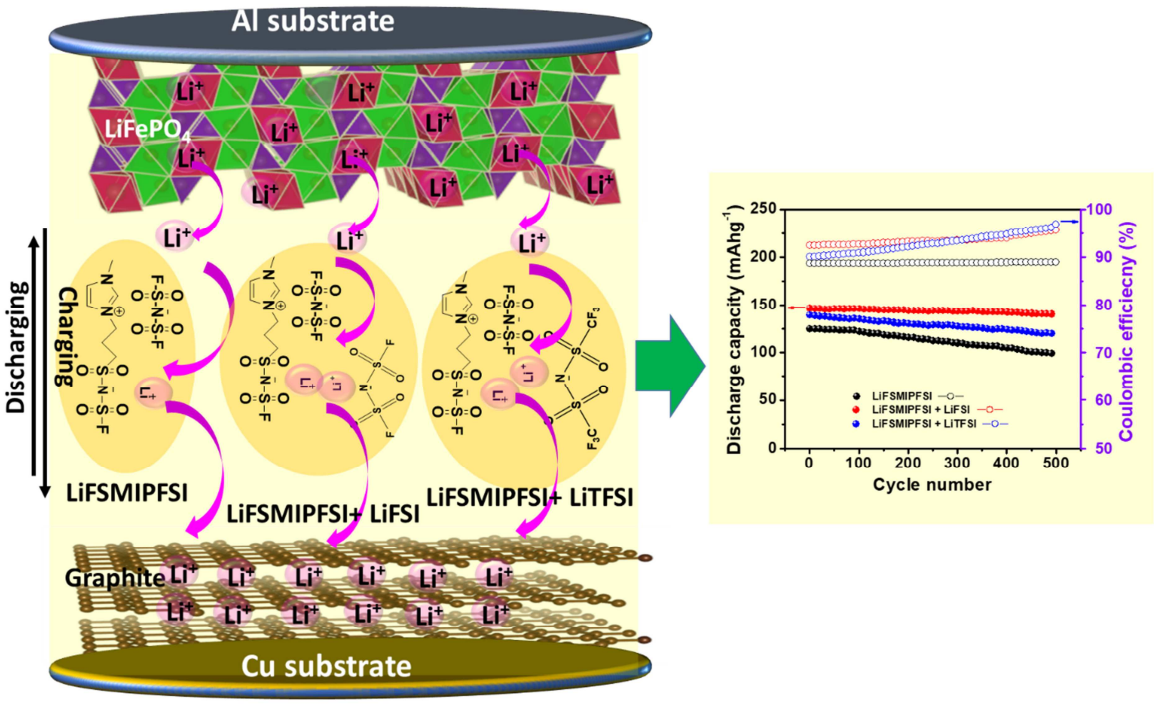

Synthesis and Electrochemical Performance of an Imidazolium Based Li Salt as Electrolyte with Li Fluorinated Sulfonylimides as Additives for Li-Ion Batteries

Faiz Ahmed, Md. Mahbubur Rahman, Sabuj Chandra Sutradhar, Nasrin Siraj Lopa, Taewook Ryu, Sujin Yoon, Inhwan Choi, Yonghoon Lee, Whangi Kim*

Department of Energy and Materials, Konkuk University, Chungju 27478, South Korea

*Author to whom correspondence should be addressed: E-Mail: wgkim@kku.ac.kr (W. Kim).

Abstract

Herein, we report the synthesis of a novel imidazolium-based ionic salt, lithium (fluorosulfonyl)((3-(1-methyl-1H-imidazol-3-ium-3-yl)propyl)sulfonyl) bis(fluorosulfonyl)imide (LiFSMIPFSI) as an electrolyte for the application in lithium-ion battery (LIB). The as-synthesized LiFSMIPFSI exhibited high purity and yield, which was characterized by various spectroscopic techniques. The LiFSMIPFSI electrolyte with a mixed solvent of ethylene carbonate (EC) and dimethyl sulfoxide (DMSO) (75:25 v/v) showed a wide electrochemical stability (ca. 4.5 V *vs.* Li/Li^+) and high thermal stability (300 ºC), good Li^+ conductivity (ca. 8.02 mS/cm at 30 ºC), and low intrinsic viscosity, which concurrently delivered a specific discharge capacity of ca. 125 $mAhg^{-1}$ at 0.1 C with the full LIB configuration of $LiFePO_4$/electrolytes/graphite. The performance of this LiFSMIPFSI electrolyte was enhanced further by the addition of conventional lithium bis(fluoro-sulfonyl)imide (LiFSI) and lithium bis(trifluoromethylsulfonyl)imide (LiTFSI) ionic salts (20% each) as additives with the specific discharge capacity of ca. 147 and 139 $mAhg^{-1}$, respectively, at 0.1 C. This is mainly due to the additional enhancement of Li^+ conductivity and its concentrations in the electrolytes induced by the additives. The LiFSMIPFSI electrolyte with LiFSI additive based LIB showed the highest cycling stability (capacity retention ca. 97%) among the electrolytes after 500 charge-discharge cycles. Thus, the present work contributes to the development of new ionic salts and its effects upon the addition of additives on LIB performance.

Keywords: Li-ion battery, imidazolium salts, additives, ionic conductivity, specific capacity.

1. Introduction

Recently, rechargeable lithium-ion batteries (LIBs) have captured an expanding range of applications as energy storage device for transportation, portable electronics, aerospace, and biomedical applications [1-2]. This is due to its high specific energy density (150 - 200 $WhKg^{-1}$) and efficiency compared to the other rechargeable batteries (e.g., lead-acid battery, nickel metal hydride battery) [3]. The theoretical energy storage capacity of a LIB is highly dependent on the ion storage capacity of electrode materials. Electrolytes do not affect the theoretical electron storage capacity of LIBs. However, an electrolyte can significantly influence the charge transport kinetics within a battery, which contemporarily affects the deliverable energy amount and the prolonged lifetime of LIBs [4,5].

Most of the commercial LIBs utilize non-aqueous electrolyte, in which lithium hexafluorophosphate ($LiPF_6$) is dissolved in a mixture of organic solvents [6,7]. Although the $LiPF_6$ electrolyte exhibit high ionic conductivity (10.7 mS/cm in a mixture solvent of ethylene carbonate (EC) with diethyl carbonate (DEC)) and relatively wide electrochemical stability window (ESW), it suffers from poor chemical and thermal stability [8,9]. Additionally, $LiPF_6$ is moisture sensitive (hydrolysis at room temperature) and produces harmful byproduct after few cycling of the battery [10]. Others commonly used non-aqueous electrolyte salts exhibited some demerits. For example, lithium perchlorate ($LiClO_4$) is moisture sensitive and explosive, lithium hexafluoroarsenate ($LiAsF_6$) is environmentally unfavorable, and lithium tetrafluoroborate ($LiBF_4$) show low ionic conductivity (4.9 mS/cm) [11-13].

Nowadays, fluorinated organic compounds have attracted significant interest to develop high voltage LIB electrolytes with good ionic conductivity and safety. Fluorinated organic compounds can exhibit wide ESW and high thermal stability due to the presence of a highly electronegative

fluorine atom [14,15]. Lithium trifluoromethanesulfonate, lithium tris(trifluoromethanesulfonyl)methide, lithium bis(perfluoroethylsulfonyl)imide, lithium nonafluorobutylsulfonyltrifluoromethyl sulfonylimide, lithium bis(fluoro-sulfonyl)imide (LiFSI), and lithium bis(trifluoromethylsulfonyl)imide (LiTFSI) are the commonly used fluorinated organic compounds as electrolytes for LIBs [16,17]. Most of these imide salts based electrolytes showed excellent thermal and oxidative stability (>5.0 V) but their ionic conductivities are generally very low (~ 3.0 mS/cm) compared to the $LiPF_6$ [8,18,19]. Whereas, both LiTFSI and LiFSI imide type electrolytes showed comparable ionic conductivity to $LiPF_6$ [20,21]. Furthermore, both of them exhibited low sensitivity to hydrolysis with enhanced thermal and ESW compared to the $LiPF_6$ [22,23]. Nevertheless, they are generally used as a co-salts or additives with other fluorinated slat type electrolytes [22,24]. This is due to their high reactivity with the Al current collector, which ultimately decrease the lifetime of LIBs.

Recently, ionic liquids (ILs) and Zwitterionic liquids (ZIL) based electrolytes have been utilized vastly to design and formulation of a high voltage, prolonged lifetime, and safer LIBs [6,23,25-30]. This can achieve by mixing an optimal amount of LiFSI or LiTFSI salts into these ILs and ZIL with/without the addition of solvents [25-30]. For example, Kerner *et al*. investigated the performance of LIBs using an ILs (1-ethyl-3-methylimidazolium FSI) with different composition of LiFSI salt as electrolyte [23]. In another report, Elia *et al*. demonstrated the application of a series of pyrrolidinium based ILs (N-butyl-N-methylpyrrolidinium TFSI, N-butyl-N-methylpyrrolidinium FSI, and N-methoxy-ethyl-N-methylpyrrolidinium TFSI together with 0.2 M LiTFSI salt as the electrolytes for LIBs [25]. All these electrolytes revealed exceptionally long cycle-life in LIBs as well as a high safety due to the formation of a stable solid electrolyte interface (SEI) layer onto the anode. This stable SEI layer hinders the additional

decomposition of electrolyte salts and stabilizes the anode. Similarly, some other reported IL-based electrolytes also exhibited long cycle-life in LIBs, including N-propyl-N-methylpyrrolidinium TFSI, *N*-alkyl-*N*methylpyrrolidinium TFSI, *N*-*n*-butyl-*N*-ethylpyrrolidinium TFSI, 1-(2-methoxyethyl)-3-methylimidazolium TFSI, and 3-(2-(2-methoxyethoxy)ethyl)-1-methylimidazolium TFSI [6,31-34]. Nevertheless, the ionic conductivity of these IL-based electrolytes is significantly dependent on temperature, which is increasing with increasing the temperature [23,25]. This is due to the high viscosity of these ILs at room temperature. Furthermore, the presence of a small amount of Li-salts into these ILs electrolytes is another possible reason for their low ionic conductivity [25]. This cannot overcome by increasing the concentration of Li-salts beyond the optimal concentration. Since a high concentration of Li-salts into these ILs will increase the net viscosity of electrolytes, which concurrently affects the net ionic conduction as well as battery performance. Thus, the preparation of ionic salts based on these imidazolium, pyrrolidinium, and piperidinium ILs is an attractive approach to develop high-performance LIBs.

In this research, we adopted the concept of the functionalization of an imidazolium ILs (3-butyl-1-methyl-1H-imidazol-3-ium bis(fluorosulfonyl)imide, BMIFSI) with lithium (fluorosulfonyl)imide to synthesize its corresponding lithium salt, lithium (fluorosulfonyl)((3-(1-methyl-1H-imidazol-3-ium-3-yl)propyl)sulfonyl) bis(fluorosulfonyl)imide, LiFSMIPFSI) as an electrolyte for LIBs. The LiFSMIPFSI electrolyte based on an EC and dimethylsulfoxide (DMSO) mixed solvent exhibited a low intrinsic viscosity at room temperature and high Li^+ conductivity. The Li^+ conductivity and the battery performance of this electrolyte were enhanced further by the addition of a small amount of LiFSI and LiTFSI as additives.

2. Experimental

2.1. Materials

Sulfurisocyanatidic chloride, LiTFSI (99.95%), LiFSI (99.9%), DMSO, EC, toluene, methylene chloride (MC), acetone, tetrahydrofuran (THF), ethyl acetate (EA), hexane, and benzene were procured from Sigma-Aldrich (St. Louis, MO, USA). 1-methylimidazole, 1,3-propane sultone, formic acid, hydrochloric acid (37%), and trifluorostibine were purchased from Alfa Aesar (Ward Hill, Massachusetts, USA). A $LiFePO_4$ coated Al foil (thickness ca. 55 μm), a CMS graphite coated Cu foil (thickness ca. 0.05 mm thickness), and a celgard separator (thickness ca. 25 μm) were purchased from MTI corporation (CA, USA). All the chemicals and reagents were used directly without further purification.

2.2. Instrumentations

Fourier-transform infrared spectra (FTIR) was recorded with a Nicolet iS5 spectrophotometer (ASB1100426, ThermoFisher Scientific, Massachusetts, USA). The structures of the as-synthesized compounds were analyzed by ^{1}H-NMR (Bruker DRX, 400 MHz) and ^{19}F-NMR (JEOL JNM-ECZ400 s/Li, 400 MHz) spectrometers, where tetramethylsilane (TMS) was used as an internal standard. DMSO-d_6, deuterated water **(**D_2O), and deuterated chloroform **(**$CDCl_3$) were used as solvents. Thermal properties were measured using a Scinco TGA-N 1000 analyzer in the temperature range from 30 to 600 ^{o}C at a heating rate of 5 ^{o}C/min under inert condition. The surface morphology and the elemental analysis were obtained with a field-emission scanning electron microscope (FE-SEM, JEOL 7401 F) and energy dispersive X-ray spectroscopy (EDS, INCAx-sight7421, Oxford Instruments), respectively. Electrochemical impedance spectra (EIS) was measured with an IM6ex, Zahner-Elektrik GmbH & Co. KG instrument (Germany) in the frequency range from 0.1 Hz to 0.1 MHz at open circuit condition with an AC amplitude of 5

mV. All the EIS spectra were fitted with an appropriate equivalent circuit model using Z-view software (version 3.1, Scribner Associates Inc., U.S.A.). Linear sweep voltammograms (LSV) and charge-discharge (CD) plots were measured with a multi-channel potentiostat/galvanostat (Ivium-n-Stat, Ivium Technologies, The Netherlands). For LSV measurement, conventional platinum (Pt), an Ag/AgCl (aq. saturated KCl), and a Pt wire were used as the working, reference, and counter electrodes, respectively. A viscometer (RheoSense, *hts*-VROCTM) was used to measure the intrinsic viscosity of electrolytes.

2.3. Synthesis of lithium (fluorosulfonyl)((3-(1-methyl-1H-imidazol-3-ium-3-yl)propyl)sulfonyl) bis(fluorosulfonyl)imide (LiFSMIPFSI)

Fig. 1 shows the stepwise reaction for the synthesis of LiFSMIPFSI. Prior to the synthesis of LiFSMIPFSI, different precursors were synthesized with high purity and yield, including sulfurisocyanatidic fluoride (FSO_2NCO), sulfamoyl fluoride (FSO_2NH_2), 1-methyl-3-(3-sulfopropyl)-1H-imidazol-3-ium chloride (MSIC), 3-(3-(chlorosulfonyl)propyl)-1-methyl-1H-imidazol-3-ium chloride (CSPMIC), and 3-(3-(N-(fluorosulfonyl)sulfamoyl)propyl)-1-methyl-1H-imidazol-3-ium chloride (FSSPMIC). The details for the synthesis of these precursors and their characterizations are shown in the supporting information (Figs. S1-S4, respectively).

For the synthesis of LiFSMIPFSI, LiFSI (12.5 mmol) was added into a solution of FSSPMIC (10.4 mmol) in 15 mL acetone and stirred for 3 hours at 25 ºC under nitrogen atmospheric condition. Then, the product was extracted with water and butyl acetate. The gel-type product was collected from the water layer after evaporating water, which was recrystallized in the form of powder with acetonitrile with the yield of ca. 50%. Finally, the as-synthesized white powder

of LiFSMIPFSI was dried in a vacuum oven for 24 h at 80 °C and stored in a glove box under the N_2 atmosphere for further use.

2.4. Preparation of electrolytes

The LiFSMIPFSI salt exhibit poor solubility in the conventional mixed solvents of EC/DEC or EC/dimethyl carbonate (DMC). Thus, for the preparation of LiFSMIPFSI (1 M) electrolyte solution, a mixed solvent of EC and DMSO (75:25 v/v) was used. 10 (0.1 M), 20 (0.2 M) and 30 (0.3M) % of LiFSI and LiTFSI were mixed individually into the as-prepared LiFSMIPFSI (1 M) electrolyte solutions as additives. All the electrolytes were prepared in a glove box under inert atmospheric conditions.

2.5. Preparation of dummy cells and coin cells

The asymmetric dummy cells were prepared by sandwiching a $LiFePO_4$ and a carbon black coated fluorine-doped tin oxide (FTO) electrodes, where Surlyn polymer film (thickness 60 μm) was used as a spacer and sealant (Fig. S5). The $LiFePO_4$/FTO electrodes were prepared by doctor blading a homemade paste of $LiFePO_4$ onto FTO electrodes (active area: 0.15 cm^2; thickness: ca. 10 μm), which were dried at 90 ^oC in vacuum. The $LiFePO_4$, carbon black, and poly(vinylidene difluoride) (PVDF) compositions in the $LiFePO_4$ paste was 86, 5, and 9 wt%, respectively. Similarly, graphite/FTO electrodes were prepared (active area: 0.15 cm^2; thickness: ca.12 μm) using a homemade paste with the graphitic carbon and PVDF compositions of 90 and 10 wt%, respectively. Prior to the sandwich, both $LiFePO_4$/FTO and graphite/FTO electrodes were dipped into the electrolyte solutions for 20 min. Then, the electrolyte solutions were injected into the

sandwiched dummy cells through the pre-drilled hole on one FTO side and sealed with scotch tape.

For the preparation of coin cells, a graphite coated Cu foil and a $LiFePO_4$ coated Al foil was used as anode and cathode, respectively. A celgard film was used as a separator. Prior assembling, both the anode and cathode were soaked into the electrolyte solutions for 20 min. The cells were assembled under the inert atmospheric conditions in a glove box and directly used for electrochemical measurements.

3. Results and discussions

3.1. NMR and FTIR characterization of LiFSMIPFSI

The chemical structure of LiFSMIPFSI was confirmed by ^{1}H and ^{19}F NMR, and FTIR spectroscopy. The ^{1}H and ^{19}F NMR spectra showed that all the protons and fluorine atoms were positioned correctly without the presence of any impurity peaks (Fig. 2a), indicating the high purity of the as-synthesized LiFSMIPFSI. The analytical data obtained from the ^{1}H and ^{19}F NMR are presented as follows:

^{1}H-NMR (DMSO-d_6; 298 K): δ = 9.2 (s, H), 7.8 (s, H), 7.7 (s, H), 4.25-4.35 (t, 2H), 3.85 (s, 3H), 2.4-2.6 (t, 2H), 2.0-2.2 (m, 2H) ppm.

^{19}F-NMR (D_2O; 298 K): δ = 52.04 (s, 2F), -126.47 (s, F) ppm.

Fig. 2 b shows the FTIR spectra of LiFSMIPFSI. For comparison, we also measured the FTIR spectra of LiFSI and LiTFSI (Fig. 2b). All the compounds showed their common FTIR characteristics peaks for S-N overtone and O=S=O (symmetric) at ca. 1640 and 1190cm^{-1}, respectively [35]. The broad peaks in the range of 3000-3700 cm^{-1} for all the compounds indicate the presence of adsorbed water molecules and N anions [36]. LiFSMIPFSI displayed the

additional FTIR peaks of =C-H, C=N, and C=C stretching at ca. 3104, 1580, and 1472 cm^{-1}, respectively [35], indicating the successful synthesis of LiFSMIPFSI.

3.2. Physicochemical properties

Fig. 3a illustrates the TGA plots of LiFSI, LiTFSI, and LiFSMIPFSI. Both LiFSI and LiFSMIPFSI exhibited two-step degradation. The fist-step weight loss for LiFSI was 6% in the temperature range from 200 to 300 ºC, while it was 40% for LiFSMIPFSI from 240 to 370 ºC. Afterwards a sharp weight loss of 80% was occurred for LiFSI up to 475 ºC, while it was ca. 20% for LiFSMIPFSI up to 650 ºC. This two step weight loss for LiFSI and LiFSMIPFSI can be attributed to the carbonization decomposition with slow kinetics of certain decomposition processes [37]. LiTFSI exhibited signle-step weight loss and highest stability with the decompisition at 320 ºC, which is consistent with a previous report [23]. The weight loss for LiTFSI was ca. 88% at 430 ºC. This indicates that LiFSMIPFSI has little lower thermal stability compared to LiFSI and LiTFSI. The thermal stability up to 240 ^{o}C for LiFSMIPFSI is high enough for the development of thermal resistive LIBs by considering the normal operation range (-40 ~ 85 ^{o}C) of LIBs. After the thermal decomposition of LiFSI, LiTFSI, and LiFSMIPFSI, the remaining residues weigh percent was ca. 11, 12, and 40%, respectively, which is possibly due to the formation of residual carbon species, which requires further depth investigation. The percentage of residual species is much higher for LiFSMIPFSI compared to LiFSI and LiTFSI. This can be ascribed to the high percentage of atomic carbon in the structure of LiFSMIPFSI compared to LiFSI and LiTFSI, which concurrently exhibit high percentage of residue. Additionally, we measured the melting temprature of LiFSMIPFSI, which was 177±2.5 ^{o}C, while it was 132-145 ^{o}C and 234 ^{o}C, respectively for LiFSI and LiTFSI [37,38].

Fig. 3b shows the dynamic viscosity *vs.* temperature plots of electrolytes in the range between 30 to 80 ºC. For comparison, we also measured the dynamic viscosities of LiFSI and LiTFSI in the same temperature range as shown in Fig. S6. The dynamic viscosity of LiFSMIPFSI (1 M) was ca. 2.20 cP at 30 ^{o}C, while it was ca. 0.75 cP at 80 ºC. In contrast, both LiFSI (1 M) and LiTFSI (1 M) exhibited little lower viscosity compared to the LiFSMIPFSI, which were ca. 1.91 and 2.05 cP, respectively, at 30 ^{o}C and ca. 0.45 and 0.55 cP, respectively, at 80 ºC. This decreasing viscosity with increasing temperature can be attributed to the reduction of the intermolecular forces between LiFSMIPFSI molecules. This is well agreed with the reported literature [25]. The dynamic viscosity for LiFSMIPFSI+LiFSI and LiFSMIPFSI+LiTFSI electrolytes with 20% LIFSI and LiTFSI was little higher (ca. 2.50 and 3.80 cP, respectively) than the pure LiFSMIPFSI electrolyte at 30 ºC. While they were ca. 1.30 and 1.95 cP, respectively, at 80 ºC. This low dynamic viscosity of all the electrolytes in a wide temperature range indicates that they are capable of conducting Li^{+} ions with high conductivity.

3.3. Electrochemical stability and ionic conductivity

Fig. 4a shows the LSV plots of LiFSMIPFSI, LiFSMIPFSI+LiFSI, and LiFSMIPFSI+LiTFSI electrolytes with 20% LIFSI and LiTFSI at a Pt working electrode in the potential range from 0 to 7.0 V (vs. Li/Li^{+}). For comparison, we also measured the LSV plots of LiFSI and LiTFSI electrolytes (1 M each) as shown in Fig. S7. LiFSMIPFSI electrolyte displayed the oxidative stability up to ca. 4.6 V. The current flow above 4.6 V indicating the degradation of LiFSMIPFSI. LiFSMIPFSI+LiFSI and LiFSMIPFSI+LiTFSI electrolytes remained stable up to ca. 5.50 and 5.70 V, respectively. While the electrochemical oxidative stability for LiFSI and LiTFSI electrolytes were ca. 4.65 and 4.75 V, respectively. This designates that both LiFSI and

LiTFSI can act as an effective inhibitor for the decomposition of LiFSMIPFSI. The electrochemical oxidative stability enhancement for LiFSMIPFSI+LiFSI and LiFSMIPFSI+LiTFSI electrolytes compared to their parent compounds can be ascribed to the widening of the energy gap between the oxidation and reduction potential of electrolyte [39] induced by the synergistic effect of LiFSMIPFSI and additives (LiFSI or LiTFSI). The oxidative potentials of all the electrolytes are well above the working potential of the high-performance $LiCoO_2$ and $LiFePO_4$ (ca. 4 and 3.5 V, respectively, *vs.* Li/Li^+) cathode [40,41]. Thus, LiFSMIPFSI, LiFSMIPFSI+LiFSI, and LiFSMIPFSI+LiTFSI are promising electrolytes for the development of high voltage LIBs.

The Li^+ conductivity of all the electrolytes was measured by EIS analyses with the asymmetric dummy cells (Fig. S5) in the temperature range between 30 to 80 ºC. The Li^+ conductivity was calculated according to the equation S1. Fig. 4b tabulates the ionic conductivities of LiFSMIPFSI, LiFSMIPFSI+LiFSI and LiFSMIPFSI+LiTFSI electrolytes with 20 wt% LIFSI and LiTFSI and the corresponding EIS spectra are presented in Fig. S8. All the EIS plots were fitted with an appropriate equivalent circuit model as shown in Fig. S8. The details for the EIS spectra can be found in the supporting information. The ionic conductivity of LiFSMIPFSI electrolyte was ca. 8.02 mS/cm at 30 ºC with the Li^+ transference number (t_{Li+}) of ca. 0.40, which is higher or comparable to many other conventional high-performance electrolytes, including $LiPF_6$ (10.7 mS/cm), $LiBF_4$ (4.9 mS/cm), $LiClO_4$ (8.4 mS/cm), and imide based electrolytes [11-13,20,21]. The ionic conductivity of LiFSMIPFSI electrolyte was increased with increasing temperature and it was ca. 8.16 mS/cm at 80 ºC. This is consistent with the variation of dynamic viscosities of LiFSMIPFSI electrolyte with temperature. The observed high Li^+ conductivity of LiFSMIPFSI electrolyte can be explained further by the charge

delocalization of $FSMIPFSI^-$ anion (Fig. S9). The charge delocalization of FSMIPFSI anion can induce to stabilize it, which concurrently decrease the association constant of ion pairing and increased the conductivity of Li^+ [42].

In contrast, both LiFSI and LiTFSI additives (20% each) enhanced the ionic conductivity of LiFSMIPFSI electrolyte. It was ca. 8.92 and 8.25 mS/cm for LiFSMIPFSI+LiFSI and LiFSMIPFSI+LiTFSI electrolytes, respectively, at 30 ºC with the t_{Li+} of 0.48, and 0.45, respectively. The ionic conductivities of LiFSMIPFSI+LiFSI and LiFSMIPFSI+LiTFSI electrolytes were increased with increasing temperature (ca. 9.17 and 8.45 mS/cm, respectively, at 80 ºC), which is consistent with the variation of their dynamic viscosities with temperature. The ionic conductivity for LiFSMIPFSI+LiFSI electrolytes with 10 and 30% LiFSI was ca. 8.10 and 8.75 mS/cm, respectively, while it was ca. 8.0 and 8.15 8.75 mS/cm for LiFSMIPFSI+LiTFSI electrolytes with 10 and 30% LiTFSI, respectively. Hereafter, 20% LiFSI and LiTFSI is considered as optimized additives concentrations and used for further studies. The improvement of ionic conductivity of LiFSMIPFSI electrolytes induced by the LiFSI and LiTFSI additives can be ascribed to the net enhancement of t_{Li+} into the resultant electrolytes, and it is consistent with the reported results [43,44]. LiFSMIPFSI+LiFSI electrolyte showed higher ionic conductivity enhancement compared to LiFSMIPFSI+LiTFSI electrolyte. This can be attributed to the lower viscosity of LiFSMIPFSI+LiFSI electrolyte compared to LiFSMIPFSI+LiTFSI electrolyte. Additionally, the smaller size of FSI anion compared to the TFSI anion can also facilitate the faster ion movement and concurrently increase the Li^+ conductivity of LiFSMIPFSI+LiFSI electrolyte. The activation energy (E_a) for the LiFSMIPTFSI, LiFSMIPTFSI+LiFSI, and LiFSMIPTFSI+LiTFSI electrolytes were ca. 3.80, 460, and 415 J/mol, respectively, which were calculated from the Arrhenius plots of the measured ionic

conductivities of the electrolytes as shown in the inset of Fig. 4(b). The low E_a of all the electrolytes compared to the reported other electrolytes [45,46] could be attributed to the weak binding energies between the Li^+ with the corresponding anions of the electrolytes and facilitates to obtain high ionic conductivity [46].

We also investigated the stability of electrolytes by measuring their ionic conductivities with the number of EIS scan at 30 ^oC. Each of the EIS spectra was measured after cyclic voltammetric (CV) measurement of the dummy cells for 10 cycles at a scan rate of 25 mV/s in the potential range between 0 to 5 V (vs. Li/Li^+). The variation of ionic conductivities with the number of EIS scan is summarized in Fig. S10. The ionic conductivities were decreased only ca. 2.75, 4.60, and 8.30% for LiFSMIPFSI, LiFSMIPFSI+LiFSI, and LiFSMIPFSI+LiTFSI electrolytes, respectively. This little variation of ionic conductivities of all the electrolytes indicating their high electrochemical stability, which is promising for the development of high voltage LIBs.

3.4. Electrochemical performance of electrolytes

The LIB performance of electrolyte was investigated with a full coin cell with the device structure of $LiFePO_4$/electrolytes/graphite. Fig. 5 (a-c) shows the CD profiles of all LIBs at 0.1, 0.2, and 0.3 C, respectively, in the potential up to 4 V. All the LIBs showed a lower difference in the CD potential or overpotential, which is favorable to obtain high energy efficiency with good reversibility [47]. The discharge specific capacity of these LIBs were calculated based on the cathode materials $LiFePO_4$ (LFP). The discharge specific capacity of LiFSMIPFSI, LiFSMIPFSI+LiFSI, and LiFSMIPFSI +LiTFSI electrolytes based LIBs were ca. 125, 147, 139 $mAhg^{-1}$, respectively, at 0.1 C. While it was ca. 120, 142, and 134 $mAhg^{-1}$, respectively, at 0.2 C and ca. 116, 136, and 128 $mAhg^{-1}$, respectively, at 0.3 C. The discharge specific capacity of all

the electrolyte based LIBs were ca. 85, 102, and 94 $mAhg^{-1}$, respectively, at 1 C (Fig. S11). For comparison, we also prepared the LIBs using LiFSI (1M) and LiTFSI (1M) in the EC/DMSO solvent (75:25 v/v) with the same device structures, which revealed the discharge specific capacity of ca. 126 and 123 $mAhg^{-1}$, respectively, for LiFSI and LiTFSI at 0.1 C (Fig. S12). This indicates that LiFSMIPFSI electrolyte can exhibit comparable electrochemical performance in LIBs. The discharge specific capacity of LiFSMIPFSI electrolyte based LIB was much lower than the theoretical capacity of LFP (170 $mAhg^{-1}$) [48]. This can be ascribed to the lower Li^+ ionic conductivity with significantly low t_{Li+} of LiFSMIPFSI electrolyte [44]. Nevertheless, the discharge specific capacity of pure LiFSMIPFSI electrolyte based LIBs are higher or comparable than the reported others LIBs as summarized in Table S1. The specific capacity of LiFSMIPFSI electrolyte based LIBs was enhanced upon the addition of LiFSI and LiTFSI additives and it is more effective for LiFSI additive. This is well matched with the variation of Li^+ ion conductivities, $t_{Li+,}$ and viscosities of the corresponding electrolytes. In can be noted that the discharge voltage of all the electrolyte based LIBs were much lower (ca. 2.75 V) than the normal operating voltage of LFP (3.2- 3.3 V) based LIBs [49]. This is possibly due to the low t_{Li+} of all the electrolytes (<0.5), which indicate a substantial contribution of anions motion in their total ionic conductivities [44]. Therefore, a concentration gradient is developed within the LIBs induces by the migration of anions and Li-ions in the opposite direction during charging and discharging. This creates a concertation overpotential and concurrently limits the operating voltage and the thickness of the electrodes [44,50]. All of these effects are responsible for low discharge specific capacity of these electrolytes in LIBs.

Fig. 5d shows the variations of the specific capacities and coulombic efficiencies *vs.* CD cycle number of all the electrolytes based LIBs at 0. 1 C and 30 ^oC. The discharge specific

capacity for LiFSMIPFSI, LiFSMIPFSI+LiFSI, and LiFSMIPFSI+LiTFSI electrolytes based LIBs was decreased of ca. 21 (99 $mAhg^{-1}$), 4 (140 $mAhg^{-1}$), and 17% (119 $mAhg^{-1}$), respectively, after 500 CD cycles. This specifies that LiFSI is an effective additive for the LiFSMIPFSI electrolyte to obtain high electrochemical performance as well as stability. The coulombic efficiency for LiFSMIPFSI, LiFSMIPFSI+LiFSI, and LiFSMIPFSI+LiTFSI electrolytes based LIBs was ca. 82, 94, and 90.0%, respectively, in the first CD cycle, which was monotonically increased to ca. 89, 95, and 97%, respectively, after CD cycling. This monotonic increased of coulombic efficiency with increasing the number of CD cycling can be attributed to the formation of a stable SEI layer onto the graphite anode induced by the electrolytes [51,52]. Nevertheless, the coulombic efficiency of LiFSMIPFSI electrolyte based LIB is only ca. 89% after CD cycling, which is much lower than the coulombic efficiency of LiFSMIPFSI+LiFSI, and LiFSMIPFSI+LiTFSI. This is possibly due to the low capability of the formation of SEI layer onto the graphitic anode induced by LiFSMIPFSI electrolyte.

The cell interface stability of LIBs based on these electrolytes was further investigated by analyzing the surface morphologies of the graphite anodes. Fig. 6 (a) shows the FE-SEM image of bare graphite and (c-d) shows the FE-SEM images of graphite anodes of LIBs based on LiFSMIPFSI, LiFSMIPFSI+LiFSI, and LiFSMIPFSI+LiTFSI electrolytes, respectively. All the LIBs graphite anodes were recovered after 500 CD cycling of the cells at 0.1 C. It revealed that all the electrolytes are capable of forming a dense and stable SEI layer onto the graphite anode. Nevertheless, the SEI layer formed onto the graphite anode enabled by the LiFSMIPFSI+LiFSI electrolyte is much thicker than the SEI layer formed by LiFSMIPFSI, LiFSMIPFSI+LiTFSI electrolytes. This SEI layer can induce to extend the stability of the electrode/electrolyte interface, which concurrently improved the stability of LIBs [10]. This is consistent with the

electrochemical cycling stability and coulombic efficiencies of the LIBs based on these electrolytes. The formation of the SEI layer was verified further by measuring the EDS elemental mapping of the corresponding graphite anodes as shown in Figs. S13-S15. The EDS elemental mapping clearly indicates the existence of high density of elemental C, O, F, S, and N in all the graphite anodes and it is higher for LiFSMIPFSI+LiFSI.

4. Conclusions

The aim of this research is to functionalized an imidazolium ILs (BMIFSI) with lithium (fluorosulfonyl)imide to prepare its corresponding ionic salts LiFSMIPFSI as an electrolyte for LIBs. The LiFSMIPFSI electrolyte showed comparable ionic conductivity with many other conventional electrolytes, high electrochemical and thermal stability, which concurrently delivered a specific discharge capacity of ca. 125 $mAhg^{-1}$ at 0.1 C in a LIB. The electrochemical performance of this electrolyte was enhanced additionally by the addition of LiFSI and LiTFSI additives, which was maximized for LiFSI additive in terms of ionic conductivity, discharge capacity, and cycling stability. Despite the good electrochemical performance of this LiFSMIPFSI electrolyte without and with additives, the safety of these electrolyte based LIBs is still a big concern for commercialization. This required further studies, which is underway of investigation in our laboratory. The present study will give a breakthrough for the development of high-performance electrolytes for LIBs based on the functionalization of others imidazolium, pyrrolidinium, and piperidinium ILs based ionic salts.

Acknowledgements

This work was supported by Konkuk University in 2018.

Appendix A. Supplementary material

Supplementary data associated with this article can be found, in the online version, at http://dx.doi.org/xx.xxxx/j. electacta.20xx.xx.xxx.

References

[1] M. M. Huie, R. A. DiLeo, A. C. Marschilok, K. J. Takeuchi, E. S. Takeuchi, Ionic liquid hybrid electrolytes for lithium-ion batteries: a key role of the separator–electrolyte interface in battery electrochemistry, ACS Appl. Mater. Interfaces 7 (2015) 11724–11731.

[2] Q. Gan, H. He, K. Zhao, Z. He, S. Liu, Preparation of N-doped porous carbon coated MnO nanospheres through solvent-free in-situ growth of ZIF-8 on $ZnMn_2O_4$ for high performance lithium-ion battery anodes, Electrochim. Acta 266 (2018) 254–262.

[3] N. Nitta, F. Wu, J. T. Lee, G. Yushin, Li-ion battery materials: present and future, Mater. Today 18 (2015) 252–264.

[4] T. R. Jow, S. A. Delp, J. L. Allen, J.-P. Jones, M. C. Smart, Factors limiting Li^+ charge transfer kinetics in Li-ion batteries, J. Electrochem. Soc. 165 (2018) A361-A367.

[5] F. Jiang, P. Peng, Elucidating the performance limitations of lithium-ion batteries due to species and charge transport through five characteristic parameters, Sci. Rep. 6 (2016) 32639.

[6] Q. Li, J. Chen, L. Fan, X. Kong, Y. Lu, Progress in electrolytes for rechargeable Li-based batteries and beyond, Green Energy Environ. 1 (2016) 18–42.

[7] K. Xu, Nonaqueous liquid electrolytes for lithium-based rechargeable batteries, Chem. Rev. 104 (2004) 4303–4418.

[8] R. Younesi, G.M. Veith, P. Johansson, K. Edstrom, T. Vegge, Lithium salts for advanced lithium batteries: Li–metal, Li–O_2, and Li–S, Energy Environ. Sci. 8 (2015) 1905–1922.

[9] J. Kalhoff, G. G. Eshetu, D. Bresser, S. Passerini, Safer electrolytes for lithium□ion batteries: state of the art and perspectives, ChemSusChem 8 (2015) 2154–2175.

[10] M. Stich, M. Göttlinger, M. Kurniawan, U. Schmidt, A. Bund, Hydrolysis of $LiPF_6$ in carbonate-based electrolytes for lithium-ion batteries and in aqueous Media, J. Phys. Chem. C 122 (2018) 8836–8842.

[11] R. Marom, O. Haik, D. Aurbach, I. C. Halalay, Revisiting $LiClO_4$ as an electrolyte for rechargeable lithium-ion batteries, J. Electrochem. Soc. 157 (2010) A972-A983.

[12] D. Aurbach, Nonaqueous Electrochemistry, CRC Press, Florida, 1999.

[13] S. S. Zhang, K. Xu, T. R. Jow, Low-temperature performance of Li-ion cells with a $LiBF_4$-based electrolyte, J. Solid State Electrochem. 7 (2003) 147–151.

[14] L. Xia, S. Lee, Y. Jiang, Y. Xia, G. Z. Chen, Z. Liu, Fluorinated electrolytes for Li-Ion batteries: the lithium difluoro(oxalato)borate additive for stabilizing the solid electrolyte interphase, ACS Omega 2 (2017) 8741–8750.

[15] Z. Zhang, L. Hu, H. Wu, W. Weng, M. Koh, P. C. Redfern, L. A. Curtiss, K. Amine, Fluorinated electrolytes for 5 V lithium-ion battery chemistry, Energy Environ. Sci. 6 (2013) 1806–1810.

[16] M. Carboni, S. Brutti, A. G. Marrani, Surface reactivity of a carbonaceous cathode in a lithium triflate/ether electrolyte-based $Li-O_2$ cell, ACS Appl. Mater. Interfaces 7 (2015) 21751−21762.

[17] V. Aravindan, J. Gnanaraj, S. Madhavi, H.-K. Liu, Lithium-ion conducting electrolyte salts for lithium batteries, Chem. Eur. J. 17 (2011) 14326–14346.

[18] A. Moretti, S. Jeong, G. A. Giffin, S. Jeremias, S. Passerini, Li-doped *N*-methoxyethyl-*N*-methylpyrrolidinium fluorosulfonyl-(trifluoromethanesulfonyl)imide as electrolyte for reliable lithium ion batteries, J. Power Sources 269 (2014) 645–650.

[19] J. C. Burns, N. N. Sinha, G. Jain, H. Ye, C. M. VanElzen, W. M. Lamanna, A. Xiao, E. Scott, J. Choi, J. R. Dahn, Impedance reducing additives and their effect on cell performance I. $LiN(CF_3SO_2)_2$, J. Electrochem. Soc. 159 (2012) A1095–A1104.

[20] M. Dahbi, F. Ghamouss, F. Tran-Van, D. Lemordant, M. Anouti, Comparative study of EC/DMC LiTFSI and $LiPF_6$ electrolytes for electrochemical storage, J. Power Sources 196 (2011) 9743–9750.

[21] S.-J. Kang, K. Park, S.-H. Park, H. Lee, Unraveling the role of LiFSI electrolyte in the superior performance of graphite anodes for Li-ion batteries, Electrochim. Acta 259 (2018) 949–954.

[22] V. Sharova, A. Moretti, T. Diemant, A. Varzi, R. J. Behm, S. Passerini, Comparative study of imide-based Li salts as electrolyte additives for Li-ion batteries, J. Power Sources 375 (2018) 43–52.

[23] M. Kerner, N. Plylahan, J. Scheers, P. Johansson, Ionic liquid based lithium battery electrolytes: fundamental benefits of utilising both TFSI and FSI anions?, Phys. Chem. Chem. Phys. 17 (2015) 19569-19581.

[24] G. G. Eshetu, S. Grugeon, G. Gachot, D. Mathiron, M. Armand, S. Laruelle, LiFSI vs. $LiPF_6$ electrolytes in contact with lithiated graphite: comparing thermal stabilities and identification of specific SEI-reinforcing additives, Electrochim. Acta 102 (2013) 133– 141.

[25] G. A. Elia, U. Ulissi, S. Jeong, S. Passerini, J. Hassoun, Exceptional long-life performance of lithium-ion batteries using ionic liquid-based electrolytes, Energy Environ. Sci. 9 (2016) 3210-3220.

[26] J. Huang, A. F. Hollenkamp, Thermal behavior of ionic liquids containing the FSI anion and the Li^+ cation, J. Phys. Chem. C 114 (2010) 21840–21847.

[27] R.-S. Kühnel, A. Balducci, Lithium ion transport and solvation in N-Butyl-N-methylpyrrolidinium Bis(trifluoromethanesulfonyl)imide−Propylene Carbonate Mixtures, J. Phys. Chem. C 118 (2014) 5742−5748.

[28] M. Yoshizawa, A. Narita, H. Ohno, Design of ionic liquids for electrochemical applications, Aust. J. Chem. 57 (2004) 139-144.

[29] A. Narita, W. Shibayama, H. Ohno, Structural factors to improve physico-chemical properties of zwitterions as ion conductive matrices, J. Mater. Chem. 16 (2006) 1475–1482.

[30] H. Ohno, M. Yoshizawa-Fujita, Y. Kohno, Design and properties of functional zwitterions derived from ionic liquids, Phys. Chem. Chem. Phys. 20 (2018) 10978-10991.

[31] B. Yang, C. Li, J. Zhou, J. Liu, Q. Zhang, Pyrrolidinium-based ionic liquid electrolyte with organic additive and LiTFSI for high-safety lithium-ion batteries, Electrochim. Acta 148 (2014) 39–45.

[32] G.-T. Kim, G. B. Appetecchi, F. Alessandrini, S. Passerini, Solvent-free, PYR_{1A}TFSI ionic liquid-based ternary polymer electrolyte systems I. Electrochemical characterization, J. Power Sources 171 (2007) 861–869.

[33] C. Sirisopanaporn, A. Fernicola, B. Scrosati, New, ionic liquid-based membranes for lithium battery application, J. Power Sources 186 (2009) 490–495.

[34] S. Ferrari, E. Quartarone, C. Tomasi, D. Ravelli, S. Protti, M. Fagnoni, P. Mustarelli, Alkoxy substituted imidazolium-based ionic liquids as electrolytes for lithium batteries, J. Power Sources 235 (2013) 142–147.

[35] D. L. Pavia, G. M. Lampman, G. S. Kriz, J. A. Vyvyan, Introduction to spectroscopy, 4th edition, Brookescole Publishers, California, 2008.

[36] J. Ha, S. Im, S. Lee, H. Jang, T. Ryu, C. Lee, Y. Jeon, W. Kim, Liquid type of fluorosulfonyl lithium salts containing siloxane for Li-ion electrolyte, J. Ind. Eng. Chem. 37 (2016) 319–324.

[37] M. Kerner, N. Plylahan, J. Scheers, P. Johansson, Thermal stability and decomposition of lithium bis(fluorosulfonyl)imide (LiFSI) salts, RSC Adv. 6 (2016) 23327–23334.

[38] M. J. Marczewski, B. Stanje, I. Hanzu, M. Wilkening, P. Johansson, ‘‘Ionic liquids-in-salt’’ – a promising electrolyte concept for high-temperature lithium batteries?, Phys. Chem. Chem. Phys. 16 (2014) 12341-12349.

[39] P. Peljo, H. H. Girault, Electrochemical potential window of battery electrolytes: the HOMO–LUMO misconception, Energy Environ. Sci. 11 (2018) 2306–2309.

[40] V. Aravindan, J. Gnanaraj, Y.-S. Lee, S. Madhavi, $LiMnPO_4$ – A next generation cathode material for lithium-ion batteries, J. Mater. Chem. A 1 (2013) 3518–3539.

[41] M. D. Bhattab, C. O’Dwyer, Recent progress in theoretical and computational investigations of Li-ion battery materials and electrolyte, Phys. Chem. Chem. Phys. 17 (2015) 4799–4844.

[42] A. Thiam, C. Iojoiu, J.-C. Leprêtre, J.-Y. Sanchez, Lithium salts based on a series of new anilinyl-perfluorosulfonamide salts and their polymer electrolytes, J. Power Sources 364 (2017) 138–147.

[43] S. C. Pang, C. L. Tay, S. F. Chin, Starch-based gel electrolyte thin films derived from native sago (Metroxylon sagu) starch, Ionics 20(2014) 1455-1462.

[44] K. M. Diederichsen, E. J. McShane, B. D. McCloskey, Promising Routes to a High Li+ transference number electrolyte for lithium ion batterie, ACS Energy Lett. 2 (2017) 2563−2575.

[45] J. F. V. Humbeck, M. L. Aubrey, A. Alsbaiee, R. Ameloot, G. W. Coates, W. R. Dichtel, J. R. Long, Tetraarylborate polymer networks as single-ion conducting solid electrolytes, Chem. Sci. 6 (2015) 5499-5505.

[46] L. Li, S. Zhou, H. Han, H. Li, J. Nie, M. Armand, Z. Zhou, X. Huang, Transport and electrochemical properties and spectral features of non-aqueous electrolytes containing LiFSI in linear carbonate solvents, J. Electrochem. Soc. 158 (2011) A74-A82.

[47] A. Eftekhari, Energy efficiency: a critically important but neglected factor in battery research, Sustainable Energy Fuels, 1 (2017) 2053–2060.

[48] Q. Zhao, Y. Zhang, Y. Meng, Y. Wang, J. Ou, Y. Guo, D. Xiao, Phytic acid derived $LiFePO_4$ beyond theoretical capacity as high-energy density cathode for lithium ion battery, Nano Energy 34 (2017) 408–420.

[49] B. Scrosati, J. Garche, Lithium batteries: Status, prospects and future, J. Power Sources 195 (2010) 2419–2430

[50] J. Jeong, H. Lee, J. Choi, M.-H. Ryou, Y. M. Lee, Effect of $LiFePO_4$ cathode density and thickness on electrochemical performance of lithium metal polymer batteries prepared by in situ thermal polymerization, Electrochim. Acta 154 (2015) 149–156.

[51] L. Suo, O. Borodin, W. Sun, X. Fan, C. Yang, F. Wang, T. Gao, Z. Ma, M. Schroeder, A. Cresce, S. M. Russell, M. Armand, A. Angell, K. Xu, C. Wang, Advanced high-voltage aqueous

lithium-ion battery enabled by “Water-in-Bisalt” electrolyte, Angew. Chem. Int. Ed. 55 (2016) 7136–7141.

[52] F. Ahmed, M. M. Rahman, S. C. Sutradhar, N. S. Lopa, T. Ryu, S. Yoon, I. Choi, S. Lee, W. Kim, Novel divalent organo-lithium salts with high electrochemical and thermal stability for aqueous rechargeable Li-Ion batteries, Electrochim. Acta 298 (2019) 709–716.

Figure captions

Figure 1. Schematic of the stepwise reactions for the synthesis of Lithium (fluorosulfonyl)((3-(1-methyl-1H-imidazol-3-ium-3-yl)propyl)sulfonyl) bis(fluorosulfonyl)imide (LiFSMIPFSI).

Figure 2. (a) ^{1}H NMR spectra (inset shows the ^{19}F NMR spectra) and (b) FTIR spectra of LiFSMIPFSI.

Figure 3. (a) TGA plots of LiFSMIPFSI, LiFSI, and LiTFSI. (b) Viscosity plots of LiFSMIPFSI (1 M) without and with LiFSI (0.2 M) and LiTFSI (0.2 M) additives in EC and DMSO (75:25 v/v) solvent.

Figure 4. (a) LSV plots (scan rate of 25 mV/s) and (b) Li^{+} conductivity *vs.* temperature plots of LiFSMIPFSI, LiFSMIPFSI+LiFSI, and LiFSMIPFSI+LiTFSI electrolytes. Inset of (b) shows the Arrhenius plots of the measured ionic conductivity.

Figure 5. Voltage profiles of $LiFePO_4$/electrolytes/graphite based LIBs coin cells at (a) 0.1 C, (b) 0.2 C, and (c) 0.3 C at 30 ^{o}C. (d) Variation of the discharge capacity and the coulombic efficiency as a function of CD cycling number of the corresponding LIBs at 0.1 C and 30 ^{o}C.

Figure 6. FE-SEM images of (a) bare graphite anode and (b-d) graphite anodes based on LiFSMIPFSI, LiFSMIPFSI+LiFSI, and LiFSMIPFSI+LiTFSI electrolytes contained LIBs, respectively. All the graphite anodes were recovered after 500 CD cycles of LIBs at 0.1 C and 30^{o}C. Insets of all images show the corresponding magnified FE-SEM images.

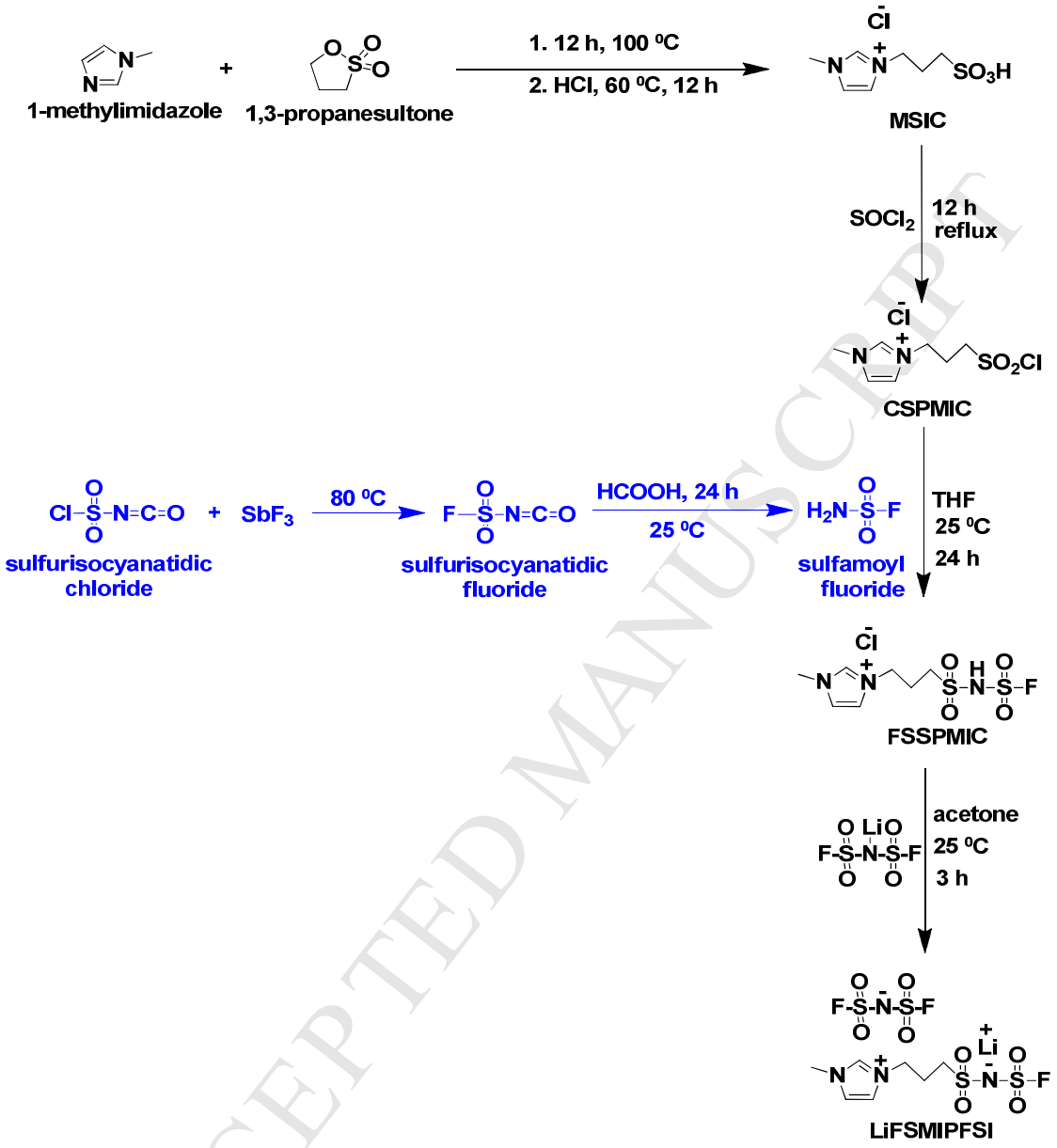

Figure 1. W.G. Kim et al.

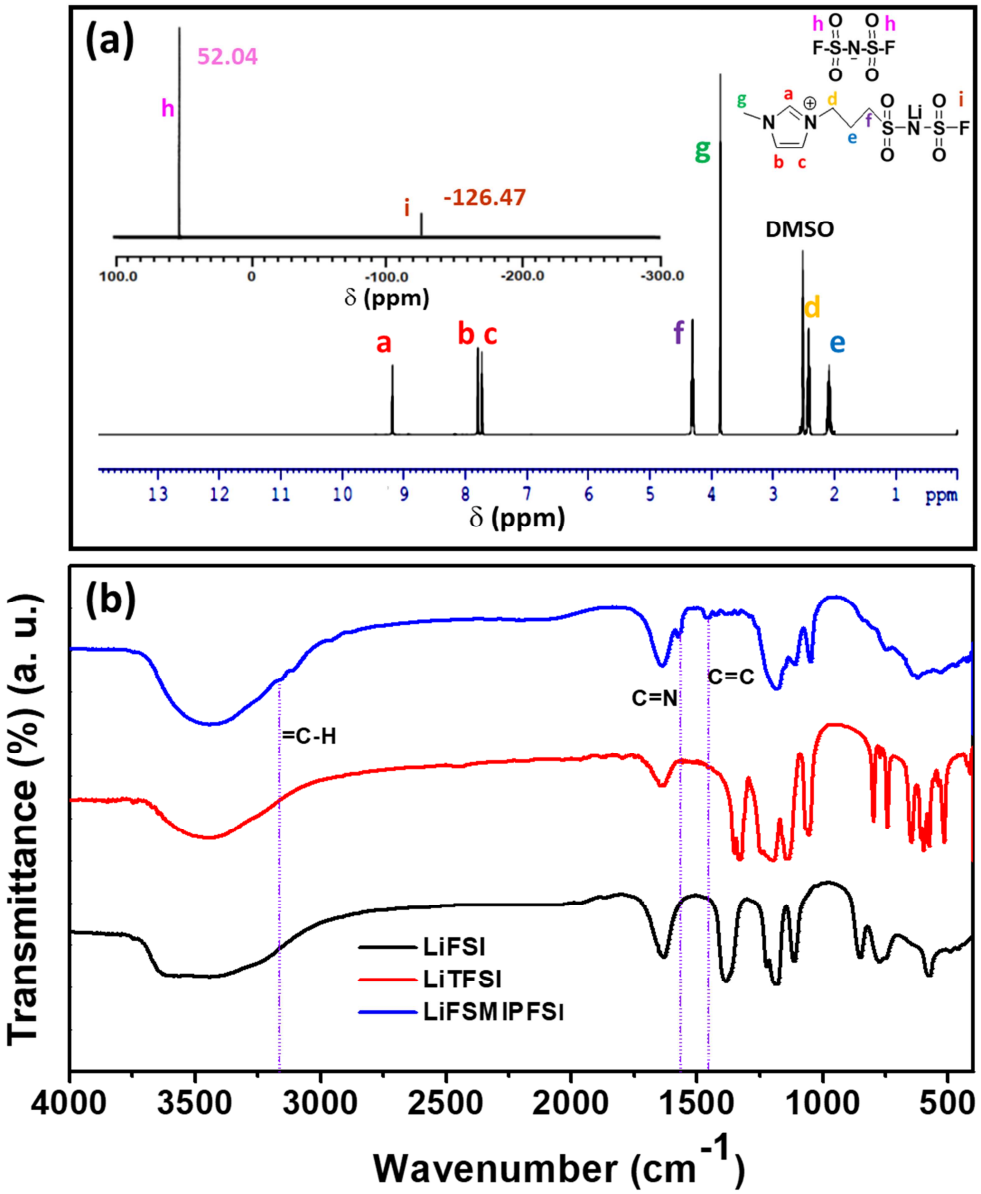

Figure 2. W.G. Kim et al.

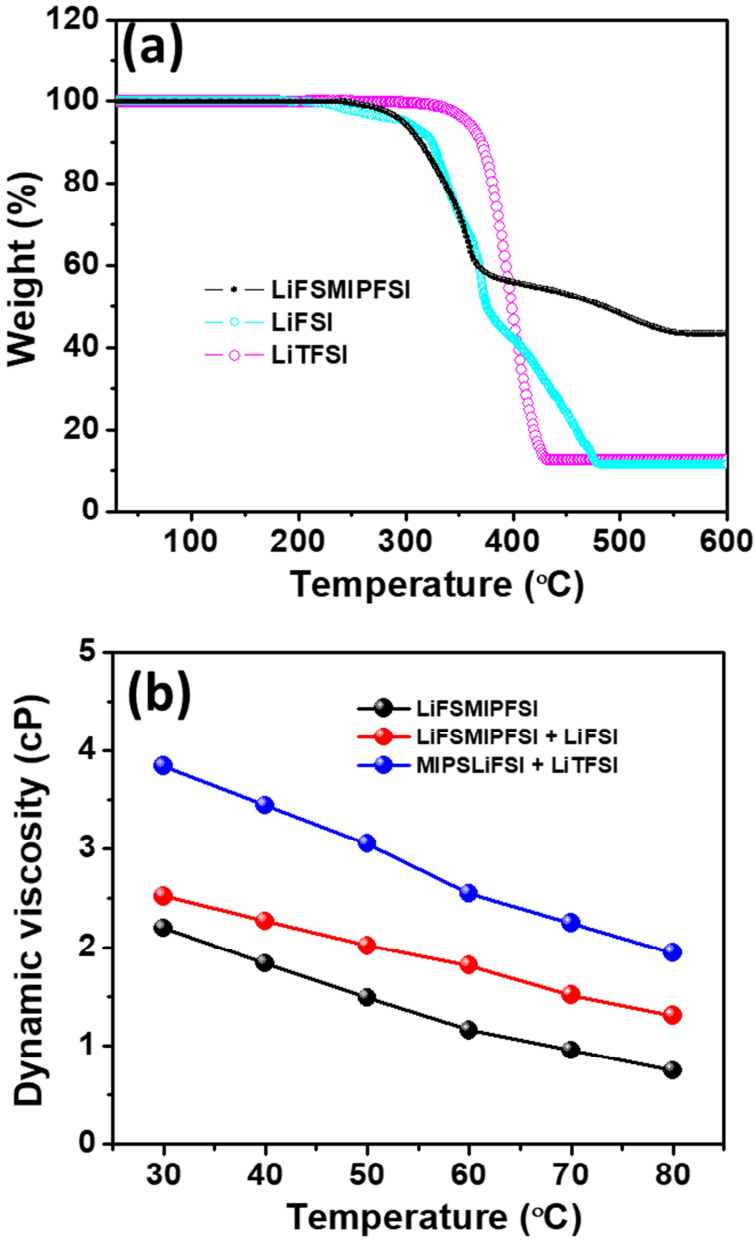

Figure 3. W.G. Kim et al.

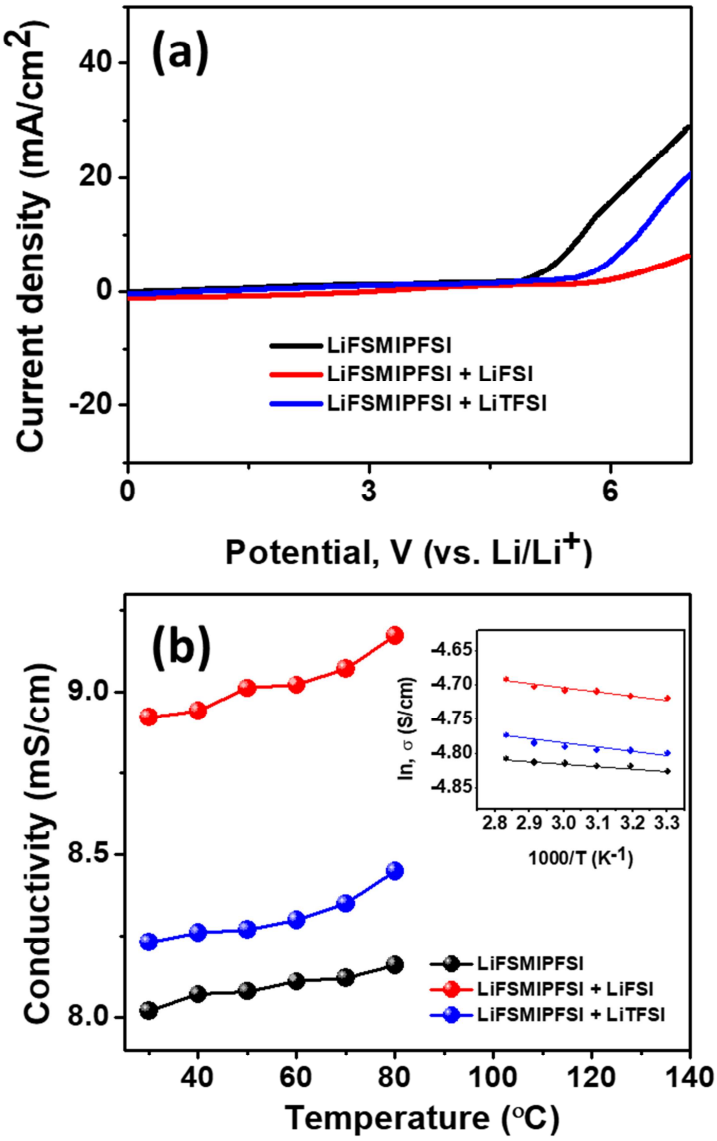

Figure 4. W.G. Kim et al.

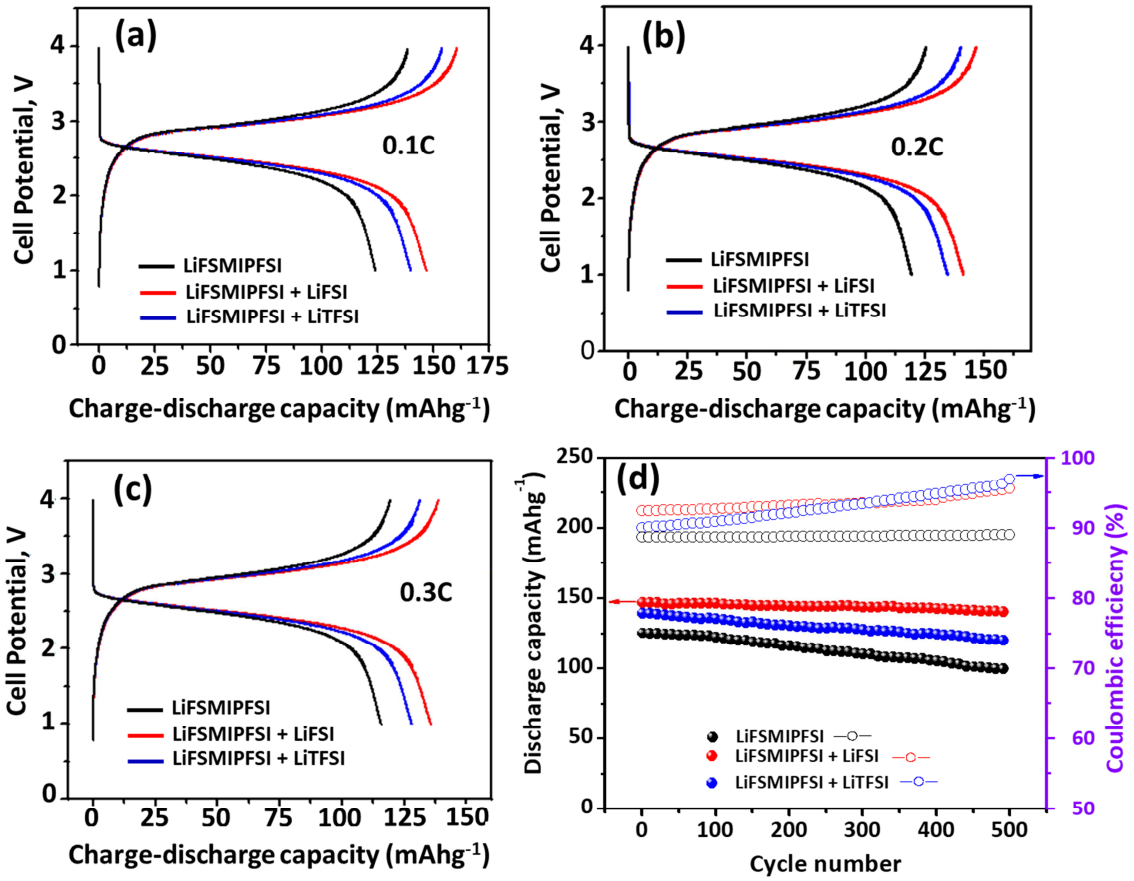

Figure 5. W.G. Kim et al.

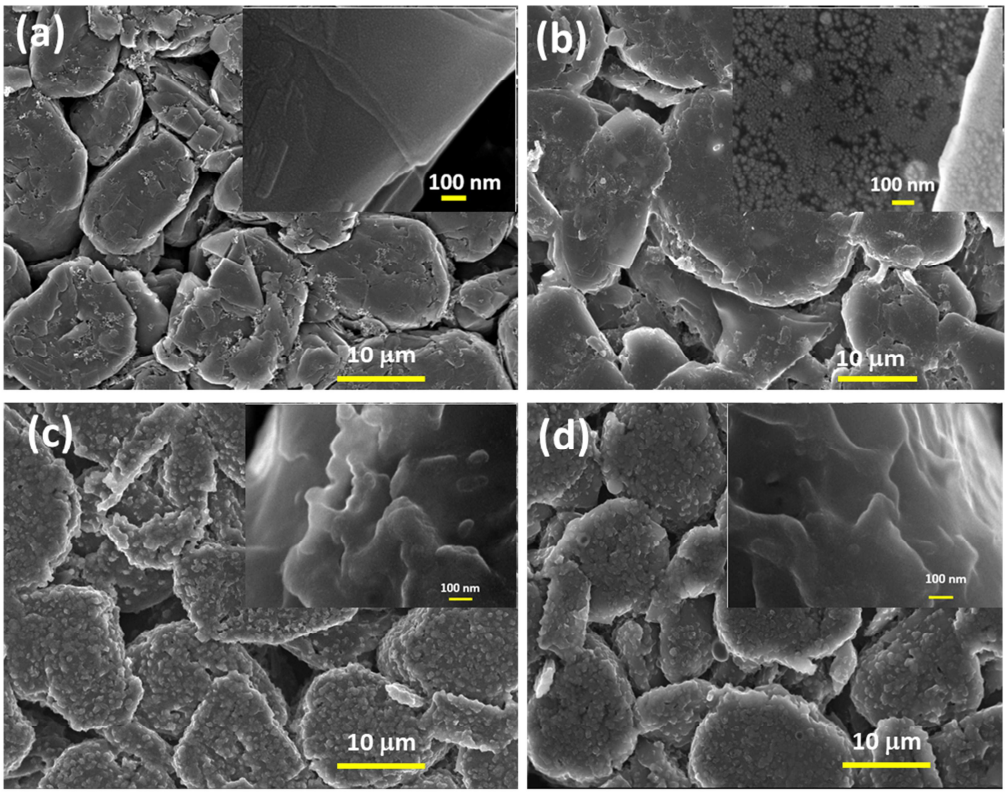

Figure 6. W.G. Kim et al.

Highlights

- Imidazolium-based ionic salt (LiFSMIPFSI) was prepared as an electrolyte for LIBs.
- LiFSMIPFSI electrolyte showed good ionic conductivity and LIB performance.
- LiFSI and LiTFSI were added as additives to enhance the performance of LiFSMIPFSI.
- LiFSMIPFSI with LiFSI additive delivered a maximum capacity of 147 $mAhg^{-1}$.
- The electrolyte without/with additives showed good capacity retention.